Shared Holes Trapped by Charge Defects in SrTiO₃

T. C. Ensign* and S. E. Stokowski†

National Bureau of Standards, Washington, D. C. 20234

(Received 6 October 1969)

Using the techniques of EPR and optical irradiation in conjunction with optical-absorption measurements, we have gained useful information about the nature of some hole centers in SrTiO₃. Primarily, we have investigated, at temperatures near 77°K, single crystals doped with aluminum. Two principal centers have been explored: (1) the Al-O⁻ center—a hole shared among the oxygens which surround Al^{3+}, and (2) the X-O⁻ center—a hole shared in a similar fashion, but more deeply trapped by a charge defect of unknown origin. The Al-O⁻ center arises after band-gap irradiation and is characterized at 77°K by the following g values and hyperfine constants: $g_{||} = 2.0137$, $g_\perp = 2.0124$, $A_{||} = 8.3 \times 10^{-4}$ cm⁻¹, and $A_\perp = 7.6 \times 10^{-4}$ cm⁻¹. The X-O⁻ center is present before optical irradiation. No hyperfine structure is observed, but the isotropic g value is 2.0130 at all temperatures from 4.2 to 300°K. An 800-nm absorption band arising after band-gap excitation has been correlated with the Al-O⁻ center. 430- and 600-nm absorption bands have been correlated with the absence of Fe^{3+} in the EPR spectrum, and a 500-nm band has also been observed. In addition, the role of iron in the photochromic processes of SrTiO₃ is presented. Finally, theoretical work utilizing the molecular orbital σ and π states in O_h symmetry has provided a firm basis for the sharing model. The experimental g values and hyperfine constants are discussed in light of this model and are found to be in good agreement.

I. INTRODUCTION

THE perovskite SrTiO₃ has been and continues to be a thoroughly explored crystal. Within it there exists an array of fascinating properties. Interest has arisen because of its high and temperature-dependent dielectric constant.[1] A structural phase transition has been explained in terms of one of the two temperature-dependent soft phonon modes.[2,3] In addition, SrTiO₃ is one of an interesting group of semiconductors which is a superconductor.[4] Its use as a host crystal for numerous impurity ions has led to a more thorough understanding of both the role of the impurities and the microscopic properties of SrTiO₃, in general. Details about the crystal structure have been provided by several EPR studies using transition-metal and rare-earth ions.[5] Optical-absorption measurements on transition-metal–doped SrTiO₃ were taken initially by Gandy[6] and later by Müller.[7] Sharp-line fluorescence has been observed in crystals doped with Cr and Mn.[8] More recently, interest in SrTiO₃ has been rekindled by Faughnan and Kiss's[9] discovery of the photochromic behavior

of this crystal—a feature which is of some practical importance.

Our interest in SrTiO₃ evolved upon observing that a particular heat treatment or Al₂O₃ doping resulted in a rose-colored crystal. Our motivation has been to determine the nature of the defects in SrTiO₃ which might account for the unique color as well as other unexplained properties of this crystal—for instance, the broad-band emission seen in undoped SrTiO₃.[10]

In the course of this study, we have encountered what, we believe, are rather unusual centers of some theoretical interest.[11] The most prominent of these consists of a trapped hole which is shared among the six oxygens surrounding an Al^{3+} impurity ion. Another center is a similarly shared hole which has been trapped by a charge defect of unknown origin. In addition to their interesting properties, these centers also play an important role in the photochromic effects observed in SrTiO₃.

In Sec. III, we present the results of the EPR and optical experiments. We describe the nature of the hole centers which we have observed and discuss their role and that of iron in the photochromic process. A theoretical model of the shared hole center is presented in Sec. IV.

II. EXPERIMENTAL

A. Samples and Sample Preparation

The samples investigated in this work were single crystals of SrTiO₃. All data were obtained for crystals grown either commercially[12] or in this laboratory by Roberts.

[1] H. E. Weaver, J. Phys. Chem. Solids 11, 274 (1959).

[2] J. M. Worlock and P. A. Fleury, Phys. Rev. Letters 19, 1176 (1967).

[3] P. A. Fleury, J. F. Scott, and J. M. Worlock, Phys. Rev. Letters 21, 16 (1968).

[4] J. F. Schooley, W. R. Hosler, E. Ambler, J. H. Becker, M. L. Cohen, and C. S. Koonce, Phys. Rev. Letters 14, 305 (1965).

[5] W. Low and E. L. Offenbacher, Solid State Phys. 17, 135 (1965).

[6] H. W. Gandy, Phys. Rev. 113, 795 (1959).

[7] K. A. Müller, in *Paramagnetic Resonance, Proceedings of the First International Conference, Jerusalem, 1963*, edited by W. Low (Academic Press Inc., New York, 1963), Vol. 1, p. 17.

[8] S. E. Stokowski and A. L. Schawlow, Phys. Rev. 178, 457 (1969).

[9] B. W. Faughnan and Z. J. Kiss, Phys. Rev. Letters 21, 1331 (1968).

[10] L. H. Grabner, Phys. Rev. 177, 1315 (1969); Y. T. Sihvonen, J. Appl. Phys. 38, 4431 (1967).

[11] T. C. Ensign, S. E. Stokowski, and T. Chang, Bull. Am. Phys. Soc. 14, 376 (1969); S. E. Stokowski and T. C. Ensign, *ibid.* 14, 376 (1969).

[12] We are grateful to Dr. D. Beals of the National Lead Co. for kindly supplying some of the samples used in this study.

In Fig. 1, we depict the ABO_3 structure characteristic of a perovskite. Of major concern to us in this study have been the oxygen octahedra which surround Ti and which comprise the simple cubic lattice with Sr at the body center of the cubic unit cell. At 107°K, $SrTiO_3$ undergoes a structure phase transition from cubic $(O_h^1, Pm3m)$ to tetragonal $(D_{4h}^{18}, 14/mcm)$.[13,14]

In this study, we have explored primarily the following crystals:

(a) Undoped $SrTiO_3$ which was heated to 1200°C and quenched in flowing oxygen. It was estimated that the time of the quench was less than 30 sec—that is, the crystal temperature fell below 850°C (the "freezing-in" temperature for the diffusion of oxygen in $SrTiO_3$)[15] within this time. This treatment resulted in a transformation of the crystal's color from water-white to rose.

(b) $SrTiO_3$ nominally doped with 0.1% Al_2O_3. These crystals were also a rose color when oxidized after crystal growth.

(c) $SrTiO_3$ containing nominally 0.1% Ga_2O_3. However, the optical-absorption results indicate that less Ga substitutes than Al.

In Table I, we list the impurity concentrations of a typical undoped crystal as obtained by an emission spectrochemical analysis. Any other cation impurities were not present in concentrations larger than $\sim 0.0001\%$ by weight, the lower limit of spectrochemical analysis.
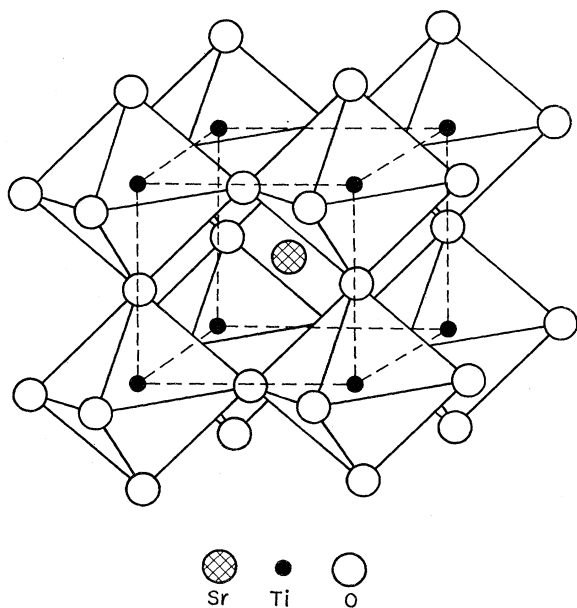

Sr   Ti   O

Fig. 1. Crystal structure of $SrTiO_3$.

[13] H. Unoki and T. Sakudo, J. Phys. Soc. Japan **23**, 546 (1967).
[14] G. Shirane and Y. Yamada, Phys. Rev. **177**, 858 (1969).
[15] A. E. Paladino, L. G. Rubin, and J. S. Waugh, J. Phys. Chem. Solids **26**, 391 (1965).

The above samples have been investigated at 300, 77, 20, and 4.2°K with additional measurements taken from 64°K (pumped liquid nitrogen) to 100°K. The majority of EPR and optical data, however, was obtained for the aluminum-doped samples at or near liquid-nitrogen temperature.

In the EPR experiment, samples of varying size were cut from the boule. These ranged from 0.2×1×6 mm at 4.2°K to 1×2×10 mm at 300°K. Larger crystals were used for the optical-absorption measurements. These samples were oriented for EPR work using x rays and the technique of Laue back reflection. Data were obtained for the magnetic field in the $(1\bar{1}0)$ and (001) planes of the crystal.

B. EPR-Optical and Optical-Absorption Experiments

In a study of this type, the final interpretation is greatly aided by the combination of various tools and/or by the correlation between them. In this study, we have combined the techniques of EPR and optical irradiation and have obtained a direct correlation with the optical-absorption measurements. This was facilitated by being able to ensure the identical experimental conditions for both experiments.

In the EPR experiment, a sample probe was employed such that coupling of the resonant cavity to the microwave system at low temperatures was accomplished via a microwave transition and coaxial line. In addition, this design allowed optical excitation from a 200-W high-pressure mercury lamp (after passing through a monochromator) to be channeled down the stainless-steel light pipe. In this way, the sample was illuminated from the top and thus remained in the dark at all other times. The details of this system are described elsewhere.[16]

Microwave saturation of the EPR centers at 77°K and below dictated the use of superheterodyne detection. The EPR spectra were recorded at X band (~ 9.5 GHz) and were calibrated in the conventional way.

A commercial double-beam spectrophotometer was used for the optical-absorption measurements. This instrument is designed such that the analyzing light passes through a monochromator before being incident on the sample. Therefore, because of the low intensity of analyzing light, we could neglect the photochromic behavior of the $SrTiO_3$ samples since their absorption was not affected during the measurement. The same

TABLE I. Spectrochemical analysis of undoped $SrTiO_3$ (impurity concentrations in percent composition by weight).

Al	0.001 –0.01	K	0.0001–0.001
Ba	0.001 –0.01	Mg	0.0001–0.001
Ca	0.001 –0.01	Mn	0.0001–0.001
Cu	0.0001–0.001	Na	0.0001–0.001
Fe	0.0001–0.001	Si	0.001 –0.01

[16] T. C. Ensign and T. Chang, Rev. Sci. Instr. **40**, 268 (1969).

samples were investigated as in the EPR experiment where, again, the major data were obtained at 77°K for the aluminum-doped crystals.

Optical bleaching was accomplished with a monochromator and high-pressure mercury lamp. For thermal bleaching, in the EPR experiment, a heater was constructed of high-resistance wire which was wrapped around the end of the cavity. The temperature, due to the relatively high heat capacity of the sample cavity, could be kept quite stable. In the optical experiment, thermal bleaching was obtained by allowing the liquid nitrogen to boil off and then monitoring the temperature. In both cases, temperature measurements were made with a copper-constantan thermocouple.

III. RESULTS

A. EPR-Optical Experiment

In this experiment, the EPR spectra of the samples studied were recorded before and after optical excitation. In Fig. 2(a), we show the first derivative of

resonance absorption prior to optical irradiation. The spectrum shown is for aluminum-doped $SrTiO_3$ at 77°K, but this signal is present in all samples mentioned in Sec. II as well as at all temperatures from 4.2 to 300°K. However, the intensity of this line is 50 to 100 times stronger for the aluminum-doped samples than for the undoped quenched samples. In addition, the temperature dependence of the linewidth is 18.3×10^{-4} T (18.3 G) at 300°K, 3.5×10^{-4} T (3.5 G) at 77°K, and 0.5×10^{-4} T (0.5 G) at 4.2°K.

This center is characterized by its positive g shift ($\Delta g = g - 2.0023 > 0$) and by its isotropy at all temperatures. For reasons which shall become apparent later, we label this the X-O^- center. It is apparently the same center as observed by Faughnan and Kiss[9,17] in their recent studies of the photochromic properties of double-doped $SrTiO_3$. A difference does exist, for in their case the X-O^- center grows after ultraviolet excitation. In our case, however, as we see in Fig. 2(b), this center actually diminishes in intensity after band-gap excitation (365 nm), and we generate in addition
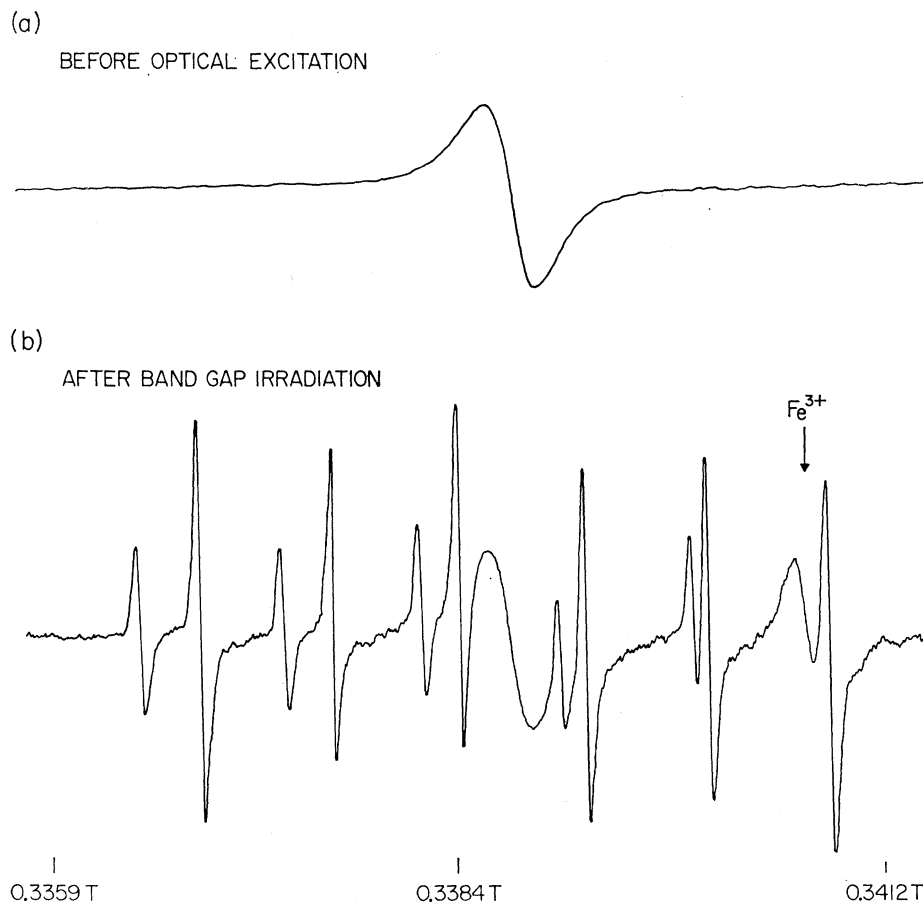
(a)

BEFORE OPTICAL EXCITATION

(b)

AFTER BAND GAP IRRADIATION

Fe^{3+}

0.3359 T	0.3384 T	0.3412 T

FIG. 2. Typical EPR spectra for $SrTiO_3$:Al_2O_3(0.1%). Crystal temperature is 77°K, microwave frequency is 9.525 GHz, and magnetic field is 5° from a cubic axis. The gain of spectrum (b) is five times that of spectrum (a) (1 T=1 tesla=10⁴ G).

[17] B. W. Faughnan and Z. J. Kiss, Bull. Am. Phys. Soc. **12**, 642 (1967).

from two to three sets of six-component hyperfine lines, depending upon crystal orientation. Furthermore, the reduction in integrated intensity of the X-O^- center is accounted for by the growth of the six-line spectra.

It will become obvious shortly that the photosensitive hyperfine spectrum arises from a hole associated with an aluminum impurity ion, and henceforth, this center will be designated the Al-O^- center. This center is present in the undoped quenched samples as well, although in these samples, as is the case of the X-O^- center, the intensity is down by two orders of magnitude.

The angular dependence of both the X-O^- and Al-O^- centers was investigated for a rotation of the magnetic field in a 5° interval about the [1$\bar{1}$0] and

[001] axes. The X-O^- center is isotropic with a g value of 2.0130. The Al-O^- center, however, is slightly anisotropic as is shown in Fig. 3. In this figure, we portray only the results for the magnetic field in a (001) plane of the crystal where the maximum information was obtained. At certain angles, the actual splitting of some of the high-field hyperfine components was not resolved experimentally. In these cases, we have anticipated the splitting in light of the angular dependence of the low-field components and in light of the appropriate theoretical expressions.

Quenching of both the X-O^- and Al-O^- centers can be accomplished with 546-nm excitation. The Al-O^- center, on the other hand, can be selectively bleached
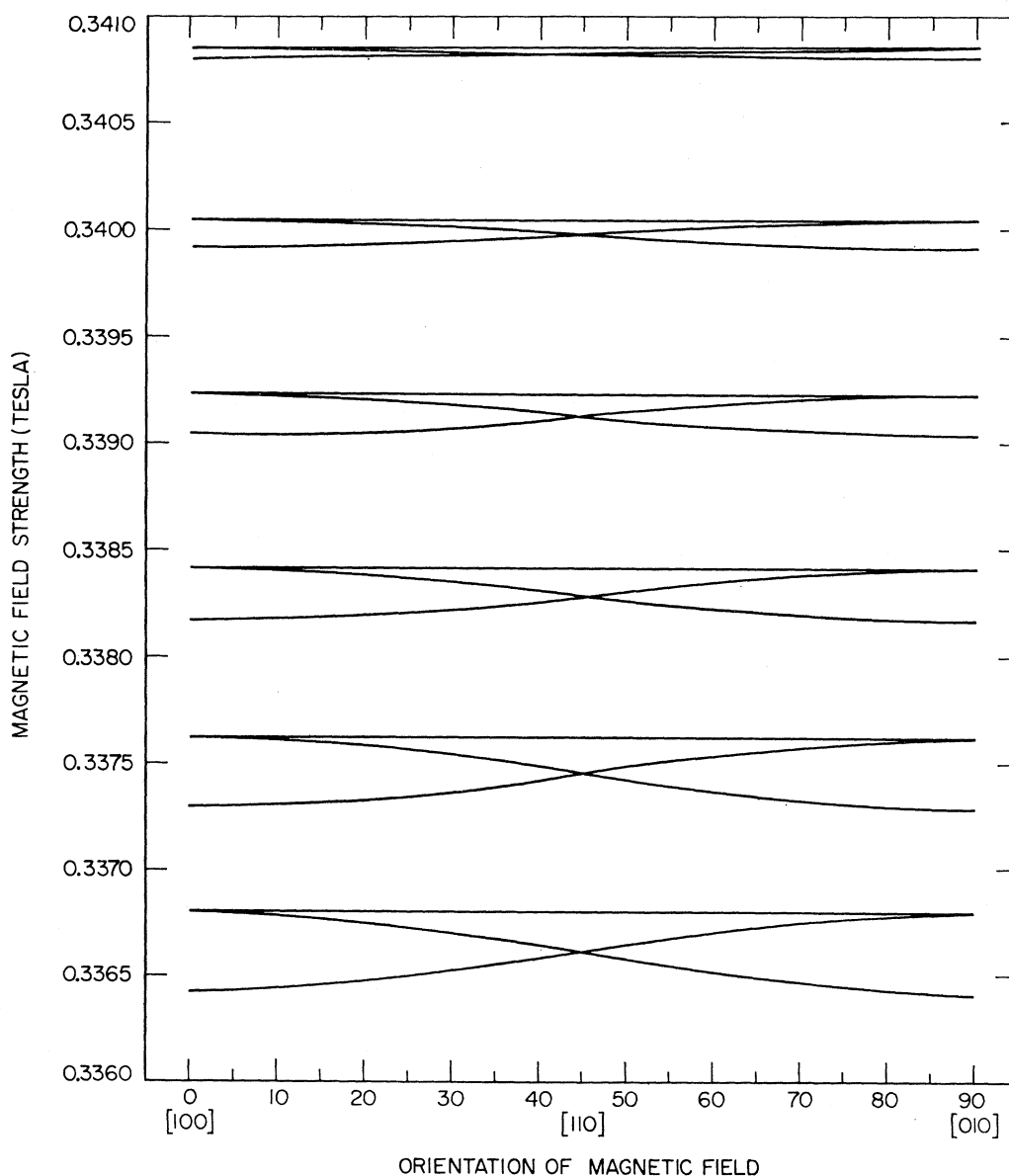

FIG. 3. Angular dependence of the Al-O^- center in SrTiO$_3$ at 77°K for the magnetic field in the (001) plane of the crystal (1 T = 10^4 G).

in either of two ways: (1) optically with 800-nm excitation, or (2) thermally by bringing the crystal temperature above 100°K. Quenching of one or all of these centers results in the growth of an Fe^{3+} impurity ion signal. As we observe in Fig. 2(b), an Fe^{3+} signal is present before bleaching, but this signal grows drastically during quenching. This impurity center has been positively identified as Fe^{3+}, since it is characterized by a g value ($g = 2.004$) and angular dependence which are consistent with Müller's work.[18] In addition, it should be noted that the bleaching process is reversible, i.e., both the X-O^- and Al-O^- centers can be regenerated with band-gap excitation. We shall now discuss the details of the important EPR centers.

1. Al-O⁻ Center

The following model has been proposed to describe the Al-O⁻ center. We believe that we have observed with EPR a hole in the $2p$ shell of an oxygen atom adjacent to Al^{3+} in a sutstitutional Ti^{4+} site. Furthermore we have evidence that this hole, which is actually an O^- species, is shared among the six octahedral oxygen orbitals.

Evidence that the Al-O⁻ center is associated with aluminum is convincing. None of the host ions (Sr, Ti, or O) are of help in understanding the hyperfine spectrum and, thus, we must look for an impurity ion with nuclear spin $I = \frac{5}{2}$ and 100% abundance. This restricts the choice to relatively few nuclei, with Al^{27} and Mn^{55} being the most likely candidates. As indicated in Table I, aluminum is a trace impurity in undoped $SrTiO_3$, and, since the Al-O⁻ spectrum grows by two orders of magnitude when 0.1% Al_2O_3 is added, we are not hesitant in correlating aluminum with the six-component spectrum. The substitution of Al^{3+} for Sr^{2+} seems unlikely, with the more probable occurrence being Al^{3+} replacing Ti^{4+}. This would leave the local site effectively negative and, thus, acting as a hole trap. In fact, the positive g shift implies a hole center. A calculation presented in Sec. IV verifies that the magnitude and sign of the g shift are consistent with the assumption that the center is a hole in the oxygen $2p$ shell.

The magnitude of the hyperfine interaction ($\sim 8 \times 10^{-4}$ cm^{-1}) is too small to be a direct hyperfine interaction. The direct hyperfine of Al^{2+}, for instance, was measured by Watkins[19] to be of the order of 450×10^{-4} cm^{-1}. This implies we are dealing with a superhyperfine interaction. The relatively isotropic hyperfine constant A (see Table II) implies that the major contribution arises from the contact term (i.e., the overlap of the hole with the $3s$ orbital of the

TABLE II. EPR results for hole centers in SrTiO$_3$.

Center	$g_{\parallel}$	$g_{\perp}$	$A_{\parallel}$ (in units of 10^{-4} cm^{-1})	$A_{\perp}$
X-O^-	2.0130±0.0001	2.0130±0.0001	⋯	⋯
Al-O^-	2.0137±0.0001	2.0124±0.0001	8.3±0.1	7.6±0.1

aluminum). Furthermore, our values of A are in very good agreement with those of Griffiths et al.[20] and Mackey[21] for aluminum-associated hole centers in quartz crystals.

The existence of three sets of six-component hyperfine lines in an arbitrary direction (as observed in Fig. 3) implies three inequivalent centers and is consistent with the Al-O⁻ center lying in tetragonal symmetry. This tetragonality could arise from the symmetry of the SrTiO$_3$ crystalline lattice, which is tetragonal below 107°K. If this is the case, the EPR spectrum should become more anisotropic as the temperature is lowered, since the tetragonal distortion of SrTiO$_3$ is temperature-dependent.[8,22] In order to test this, the Al-O⁻ center was created at 77°K prior to dropping the temperature to 20°K. At liquid-hydrogen temperature, this center was still observed, but it was found to possess the identical properties at 20°K as at 77°K (i.e., the g values and A values remained constant). Thus, we conclude that the tetragonal field arises from a temperature-independent local distortion about the Al^{3+} ion. A possible situation is a displacement of the Al^{3+} ion along one of the cubic axes. This is reasonable, since the smaller ionic radius of Al^{3+} (0.51 Å) implies that it fits loosely in the Ti^{4+} site (0.68 Å).

In Table II, we present the important experimentally measured parameters: $g_{\parallel}$, $g_{\perp}$, $A_{\parallel}$, and $A_{\perp}$. Since the oxygen site has D_{4h} symmetry, localization of the hole on a single oxygen ion would give rise to g values reflecting larger anisotropies than are apparent in our case. In addition, it can be shown that localization requires that $g_{\parallel}$ be very close to the free-electron value.[23] There exist numerous examples of localized hole centers in various host crystals of which we cite three: (1) Kasai's[23] observation of holes captured at Li acceptor levels in ZnO ($g_{\parallel} = 2.0026$, $g_{\perp} = 2.0254$), (2) O'Brien's[24] discussion of aluminum-associated hole centers in smoky quartz ($g_{\parallel} = 2.00$, $g_{\perp} = 2.06$), and (3) the study by O'Mara et al.[25] of trapped holes in MgO ($g_{\parallel} = 2.0033$,

[18] K. A. Müller, Helv. Phys. Acta **31**, 173 (1958).

[19] G. D. Watkins, in *Proceedings of the Seventh International Conference on the Physics of Semiconductors: Radiation Damage in Semiconductors* (Academic Press Inc., New York, 1965), Vol. 3, p. 97.

[20] J. H. E. Griffiths, J. Owen, and I. M. Ward, in *Report of the Bristol Conference—Defects in Crystalline Solids* (The Physical Society, London, England, 1955), p. 81.

[21] J. H. Mackey, J. Chem. Phys. **39**, 74 (1963).

[22] K. A. Müller, W. Berlinger, and F. Waldner, Phys. Rev. Letters **21**, 814 (1968).

[23] P. H. Kasai, Phys. Rev. **130**, 989 (1963).

[24] M. C. M. O'Brien, Proc. Roy. Soc. (London) **A231**, 404 (1955).

[25] W. C. O'Mara, J. J. Davies, and J. E. Wertz, Phys. Rev. **179**, 816 (1969).

$g_\perp = 2.0386$). It is interesting to note that our g values fall in an intermediate region between those for a localized hole.

Consideration of gallium-doped $SrTiO_3$ offers additional evidence for our interpretation. In this case, a photosensitive spectrum arises which is slightly different from aluminum-doped and undoped quenched $SrTiO_3$. An eight-component spectrum is generated with band-gap excitation. This spectrum is centered near $g = 2.015$ and can be accounted for quite well in terms of the interaction of a $2p$ hole on the oxygens and the nuclear spin ($I = \frac{3}{2}$) of both gallium isotopes (Ga^{69} and Ga^{71}). That is, the correct number of lines and relative intensity (3:2) is observed experimentally.

2. X-O⁻ Center

Since the X-O^- center has a g shift of the same sign and magnitude as the Al-O^- center, one is led to propose a similar holelike center in this case. Some differences are apparent. The isotropy again implies sharing, but the absence of tetragonal splitting implies that the hole trap remains in cubic symmetry. Furthermore, the X-O^- center is a deeper hole trap than the Al-O^- center, since it is stable at all temperatures from 4.2 to 300°K. Identification of the hole trap itself has been difficult, particularly since no associated hyperfine structure is observed. At 4.2 and 20°K, where the linewidth of the X-O^- center narrows appreciably, satellites are observed. Unfortunately, the experiment reveals that these satellites are not part of the X-O^- center (i.e., they are affected differently by optical excitation). Two additional curious facts exist. First, the intensity of the X-O^- center is dependent upon aluminum doping, and, second, the g value, within the experimental errors, is the average of $g_\parallel$ and $g_\perp$ of the Al-O^- center.

Various possibilities have been proposed to account for the X-O^- center, but none is totally consistent with experiment and/or theory. It has been proposed that the hole is trapped by the Al^{3+} as in the case of the Al-O^- center, but that it occupies a nonbonding or weakly bonding state. This model accounts for numerous experimental facts; however, a theoretical calculation, the details of which are presented in Sec. IV, leads to g values which are nowhere near the experimental numbers. Thus, the X-O^- center is not another state of the Al-O^- center.

Another possibility is that the hole is trapped by a lattice defect other than Al^{3+}. Iron, as we see from Table I, is a logical candidate. Fe^{4+} (or a higher valence state) can be discarded, since this ion would not act as a hole trap in $SrTiO_3$. Trapping a hole around Fe^{2+} seems unlikely since one would expect Fe^{3+} to result. Furthermore, no evidence for Fe^{2+} in a cubic site has been observed. Fe^{3+} is a possibility, but the absence of the $\frac{1}{2} \leftrightarrow -\frac{1}{2}$ cubic Fe^{3+} transition in the presence of the X-O^- center introduces a serious problem with this

model. If Fe^{3+} existed in a low-spin state,[26] however, we could explain the absence of the normal EPR spectrum.

Of course, there exist other defects in $SrTiO_3$ in addition to iron and aluminum. A visible hyperfine structure would certainly aid in the interpretation, but since none is observed one is forced to speculate. First, the hole trap (probably a trivalent ion in the Ti^{4+} site or a monovalent ion in the Sr^{2+} site) could possess nuclear spin $I = 0$. In light of Table I, with the addition of Sr, Ti, and O, we are left with no candidates in this group. Second, the hole trap could be an ion which has a low-abundant isotope with $I \neq 0$. In addition to iron, silicon would be a possibility. Third, we could consider an ion with $I \neq 0$, but in this case the magnitude of the superhyperfine interaction must be of the order of the linewidth. At 20 and 4.2°K, this implies a hyperfine interaction less than 0.5×10^{-4} cm⁻¹. There exist numerous impurity ions in $SrTiO_3$, for instance, the alkali metals (K and Na) which would be included in this category.

Another type of defect in $SrTiO_3$ which could act as a hole trap would be a Sr or Ti vacancy. In either case, the requirement for a deep trap would be satisfied; however, in Sec. IV, it is shown that the larger charge deficiency would probably lead to a theoretical g shift smaller than the experimental value.

An electron trap (for instance, an electron in an oxygen vacancy) was first suggested as the origin of the X-O^- center. However, the sign and magnitude of the g shift cannot be accounted for in this case, even in light of configurational mixing.[27] Furthermore, the symmetry of an oxygen vacancy is such as to lead to large anisotropies in the g value.

In conclusion, although the exact identity of the X-O^- center is still unknown, the evidence does support its being a hole center and not an electron trap as has been suggested by Faughnan and Kiss.[9]

3. Additional Centers

At low temperatures, an additional more complex spectrum can be created with band-gap excitation. This spectrum is particularly intense at 4.2 and 20°K, but it can also be weakly observed as high as 64°K. The multiline spectrum which appears is quite anisotropic with a g value greater than 2.0023. The center or centers responsible for this spectrum possess bleaching properties which differ from the Al-O^- and X-O^- centers. That is, this spectrum is quenched most efficiently with 1000-nm irradiation. Further data at 64°K, where both the complex spectrum and the Al-O^- center are observed simultaneously, imply a temperature-dependent competition in the formation of these centers. Accordingly, the data imply that the complex

[26] V. G. Bhide and H. C. Bhasin, Phys. Rev. **159**, 586 (1967).
[27] R. H. Bartram, C. E. Swenberg, and S. Y. La, Phys. Rev. **162**, 759 (1967).

multiline spectrum predominates at 4.2 and 20°K, thus, explaining why the Al-O⁻ center cannot be generated at these temperatures. At 77°K, the center or centers responsible for the complex spectrum thermalize and, thus, the Al-O⁻ center can form.

Throughout this study, iron has made its presence known. Understanding its exact role has been difficult, and a few facts will be presented to aid in the later interpretation. In Fe-doped SrTiO₃, the typical cubic and axial spectra are observed. Interestingly, when this crystal is quenched in flowing O_2, as described in Sec. II, the axial spectrum increases. In addition, the Fe^{3+} signal in Al-doped samples is more intense upon bleaching than in the undoped quenched samples. Furthermore, no X-O⁻ center is observed in Fe-doped SrTiO₃, quenched or unquenched, with or without band-gap excitation. The X-O⁻ center, however, is present in double-doped SrTiO₃:Mo,Fe.[9]

FIG. 4. Optical absorption of SrTiO₃:Al₂O₃ (0.1%) at 77°K. Curve 1—before optical irradiation, curve 2—after 365-nm irradiation, curve 3—after 546-nm irradiation.

TABLE III. Summary of EPR and optical results for Al-doped and O₂-quenched SrTiO₃.

Irradiation (in nm)	Temperature (in °K)	Optical (in nm)	EPR
None	77	485, 430, and 600 present	X-O⁻ present
Band-gap	77	800 appears	Al-O⁻ appears X-O⁻ decreases
546	77	485 and 800 bleached 430 and 600 decrease	X-O⁻ and Al-O⁻ bleached Fe^{3+} appears
800	77	800 bleached	Al-O⁻ bleached
None	>100	800 bleached	Al-O⁻ bleached
Band-gap	4.2	950 broad band appears	Anisotropic, multiline spectrum appears

B. Optical-Absorption Experiment

Concurrently with the EPR experiment, we have investigated the optical-absorption spectra of Al-doped, Ga-doped, and O₂-quenched SrTiO₃. We find that light and temperature effect the absorption bands present in these samples, and, furthermore, we find a strong correlation between the optical and EPR results.

The rose coloration of the SrTiO₃ samples is caused by an absorption band peaking at 485 nm with a shoulder at 600 nm, as shown in Figs. 4 and 5. When Al-doped SrTiO₃ at 77°K is exposed to light of energy near the band gap ($E>3.0$ eV), an additional band is generated at 800 nm, shown by curve 2 in Fig. 4. However, in the undoped treated SrTiO₃, band-gap light has no effect. Upon exposure of the samples to 546-nm light from a mercury arc, the 485- and 800-nm bands are bleached and two bands at 430 and 600 nm
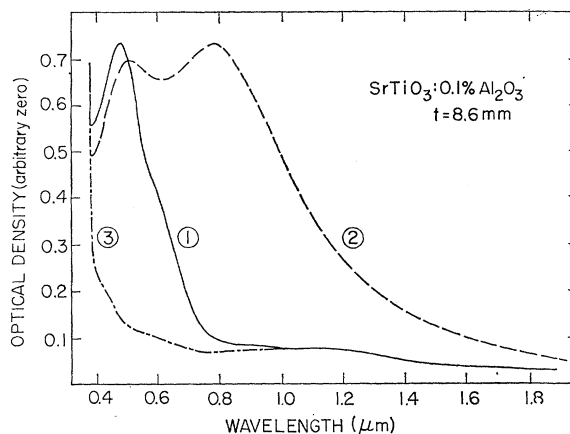
are left. We shall now discuss the properties of each absorption band in turn, and then correlate the EPR and optical results. This correlation is summarized in Table III.

1. 800-nm Band

This broad band is observed only in the Al-doped SrTiO₃ crystals, is created by band-gap light, and can be bleached by light in the wavelength range of 500–900 nm. The bleaching process is reversible (i.e., this band can be recreated by re-exposing the sample to band-gap light). The 800-nm band can also be quenched by raising the crystal temperature above 100°K. Upon comparing the properties of this band to those of the Al-O⁻ EPR spectrum, we see that they are identical. Thus, we assign the 800-nm absorption to the Al-O⁻ center. Since the EPR results indicate that the concentration of Al-O⁻ centers in the undoped quenched samples is
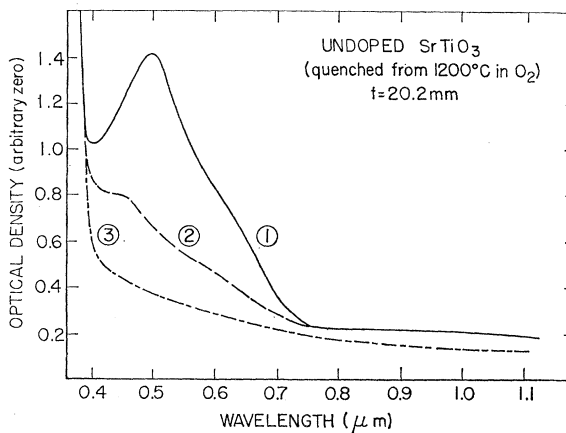

FIG. 5. Optical absorption of undoped SrTiO₃ which has been quenched from 1200°C in O₂. Crystal temperature is 77°K. Curve 1—before optical irradiation, and curve 2—after 546-nm irradiation. For comparison, the optical absorption of an untreated sample is shown by curve 3.

50 to 100 times smaller than in Al-doped $SrTiO_3$, we would not expect to see the 800-nm band in the former case. This agrees with experiment.

2. 430- and 600-nm Bands

It has been determined that these two bands are associated with the same center, since they are affected by light and temperature in the same manner and are always found with the same relative intensity. These absorption bands are usually masked by the 485-nm absorption band; however, as evident in Fig. 5, a shoulder can be discerned at 600 nm even when the 484-nm peak is present. These bands have approximately the same intensity in both Al-doped and O_2-quenched $SrTiO_3$. They can be partially bleached by 450- to 600-nm light at 77°K. However, these absorption bands can never be completely bleached. In addition, the bleaching process is more complete in the Al-doped $SrTiO_3$ than in the O_2-quenched $SrTiO_3$; the absorption is about 5 to 6 times greater in the treated samples than in the Al-doped crystals. The original intensity of the 430- and 600-nm bands can be regained either by exposure to band-gap excitation or by raising the temperature to 300°K.

This absorption is very similar to that observed by Gandy[6] in Fe-doped $SrTiO_3$. These bands also closely resemble the photo-induced absorption observed by Faughnan and Kiss[9] in Mo- and Fe-doped $SrTiO_3$.

From our work and that of Faughnan and Kiss, we see that the 600- and 430-nm bands are correlated with the absence of Fe^{3+} in the EPR spectrum. Thus, the absorption is associated with a center formed when the valence of Fe^{3+} is changed.

3. 485-nm Band

This absorption band actually peaks at 500 nm once the 430- and 600-nm bands are subtracted off. It is equally intense in both the Al-doped and O_2-quenched samples. Bleaching of this band at 77°K is accomplished with light in the 450–800 nm range. Exposure to band-gap excitation regenerates this absorption, but it also can be reformed by bringing a bleached crystal to 300°K. Recovery is attained in about 30 min at room temperature, but this time is reduced considerably by raising the temperature to about 60–80°C. This can be compared to the 430- and 600-nm bands which recover rapidly at about 10–20°C. In addition, the 500-nm band can be bleached more easily than the 430- and 600-nm bands. These results indicate that the 500-nm and 430-, 600-nm absorptions belong to two different centers, even though, to a certain extent, they behave similarly.

In comparing the properties of the 500-nm band with those of X-O^- EPR centers, we observe at first glance a one-to-one correspondence (i.e., they have the same dependence on light and temperature). However, the

EPR experiment reveals that the X-O^- center increases with Al doping by two orders of magnitude, whereas the intensity of the 500-nm band remains about constant in both Al-doped and undoped quenched $SrTiO_3$. Thus, the origin of this band is still unknown.

4. Other Absorption Bands

At 4.2°K, exposure of Al-doped $SrTiO_3$ to band-gap irradiation results in the appearance of a broad band peaking at 950 nm. This band apparently consists of bands at 600, 800, and 1000 nm. These bands appear to be associated with the anisotropic multiline EPR spectrum which is created at low temperatures. However, a detailed study of these additional centers has not been initiated.

C. Discussion

At this point, we shall concentrate on understanding the role which iron plays in the photochromic behavior of $SrTiO_3$. As we have indicated earlier, iron is very important in the charge transfer processes occurring in this crystal.

Before considering iron in the present context it is necessary to consider some of the previous work on $SrTiO_3$:Fe. Müller[18] reported that Fe-doped $SrTiO_3$ was characterized by an EPR spectrum due to Fe^{3+} in a Ti^{4+} site with no nearby compensation. Later, Kirkpatrick et al.[28] observed that some of the Fe^{3+} has local compensation in the form of a nearest-neighbor oxygen vacancy, subsequently labeled by V_0. The existence of this Fe^{3+}-V_0 complex was confirmed by Bhide and Bhasin[26,29] in Mössbauer experiments. Upon reduction of the $SrTiO_3$ samples, they observed conversion of some Fe^{3+}-V_0 into Fe^{2+}-V_0. They also worked with Co^{57}-doped $SrTiO_3$ and were able to detect Fe^{3+} in a cubic site plus an additional line which they assigned to Fe^{3+} in a low-spin state (configuration $3d^5$, t_2^5, $S = \frac{1}{2}$). However, low-spin Fe^{3+} is probably not an equilibrium state in $SrTiO_3$, since it can decay to high-spin Fe^{3+} (configuration $3d^5$, $t_2^3 e^2$, $S = \frac{5}{2}$). Its existence in the Mössbauer spectrum only means that its lifetime is longer than the lifetime of the excited nuclear state of Fe^{57} ($\sim 10^{-7}$ sec). Is is interesting to note that the ratio of low-spin-to–high-spin Fe^{3+} in the Mössbauer spectrum depends upon the heat treatment given to the sample. This indicates that the charge state of the initial cobalt ion can be changed by heat treatment. A similar effect could be present in $SrTiO_3$ doped with other transition metal ions.

Of course, there is the possibility that Fe^{4+} could appear in the Mössbauer spectrum. From Watson's[30]

[28] E. S. Kirkpartick, K. A. Müller, and R. S. Rubins, Phys. Rev. 135, A86 (1964).
[29] V. G. Bhide and H. C. Bhasin, Phys. Rev. 172, 290 (1968).
[30] R. E. Watson, Phys. Rev. 118, 1036 (1960); 119, 1934 (1960); L. R. Walker, G. K. Wertheim, and V. Jaccarino, Phys. Rev. Letters 6, 98 (1961).

values of $|\psi(0)|^2$ for the $3d^4$ configuration, the isomer shift for Fe^{4+} is estimated to be greater than -1.4 mm/sec relative to 310 stainless steel. However, such a line was not observed by Bhide and Bhasin.[26,29] On the other hand, the concentration of Fe^{4+} may have been too low for this valence state to be detected.
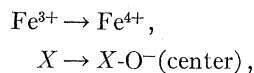
Gandy[6] subjected Fe-doped SrTiO₃ to various heat treatments, and he observed that the 430- and 600-nm absorption bands increase upon oxidation of the crystals and decrease upon reduction. These results indicate that the absorptions are due to an oxidized state of iron.

In Faughnan and Kiss's experiments,[9] irradiation of SrTiO₃:Mo and Fe crystals with blue light enhanced the 430- and 600-nm absorptions. Coincident with this was a decrease in the cubic Fe^{3+} and Fe^{3+}-V_0 EPR signals and the appearance of the X-O^- center. Thus, they have suggested the formation of Fe^{4+} as being responsible for the visible absorption in Fe-doped SrTiO₃. We, however, feel that the existence of Fe^{4+} in SrTiO₃ is still open to question since no definitive evidence for it has been found. Notwithstanding, Fe^{4+} does fit the model quite well, thus, we will assume its presence in SrTiO₃. The charge transfer processes occurring upon exposure to blue light can be summarized by the following reactions:

$$Fe^{3+} \to Fe^{4+},$$
$$Fe^{3+}\text{-}V_0 \to Fe^{2+}\text{-}V_0,$$
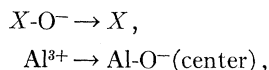$$Mo^{6+} \to Mo^{5+},$$
$$X \to X\text{-}O^-.$$
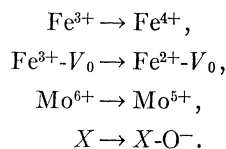
The photochromic effects investigated in our work are very similar to those observed by Faughnan and Kiss, although there exist some differences. First, the crystals studied in our work were not intentionally doped with iron or a donor impurity. Thus, we are dealing with a lower concentration of centers than in the case of double-doped SrTiO₃. For example, the absorption intensity of the 430- and 600-nm bands indicates that in our case there is about 1/50 of the Fe^{4+} observed by Faughnan and Kiss. Second, in our samples we observe a 500-nm band before optical excitation. This band was not detected in the double-doped samples. Our results can be summarized by the following reactions:
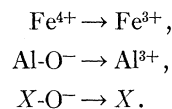
(a) Al doping or O_2 quenching:

$$Fe^{3+} \to Fe^{4+},$$
$$X \to X\text{-}O^-(\text{center}),$$

(b) band-gap excitation:

$$X\text{-}O^- \to X,$$
$$Al^{3+} \to Al\text{-}O^-(\text{center}),$$

(c) 546-nm bleaching:

$$Fe^{4+} \to Fe^{3+},$$
$$Al\text{-}O^- \to Al^{3+},$$
$$X\text{-}O^- \to X.$$

Since charge neutrality must be retained in the crystal, an inspection of the above charge transfer processes indicates the necessity for introducing at least one additional center. This center, prior to 546-nm bleaching, could be either an empty hole trap or a filled deep electron trap. In addition, this trap could account for the 500-nm absorption. One possibility for a deep electron trap is a Ti^{3+}-V_0 complex, although this center would be paramagnetic.

Of some interest is the effect of O_2 quenching or Al doping on SrTiO₃. These treatments apparently result in the disappearance of Fe^{3+} and the addition of the X-O^- center as represented in the above charge transfer reactions. It is a curious fact that these two vastly different sample treatments give rise to the same defect centers.

It is an important clue, we feel, that doping with a single transition metal does not lead to the X-O^- center in contrast to doping with Al. This may be reasonable, however, because transition-metal ions can exist in different charge states. Aluminum, on the other hand, is expected to be only in the 3+ state, and, thus, we might expect a difference in the way in which Al-doped SrTiO₃ is compensated. Infrared studies have established that $(OH)^-$ exists in larger concentrations in Al-doped SrTiO₃ than in crystals doped with a transition metal (Fe, for instance).[31] Thus, $(OH)^-$ may be important not only in understanding Al doping, but also in explaining the heat treatment. For instance, it is possible in undoped untreated SrTiO₃ that nearest-neighbor $(OH)^-$ compensates Al^{3+}. When the sample is O_2-quenched, the $(OH)^-$ migrates away, thus, allowing Al^{3+} to become a hole trap. Of course, oxygen vacancies and other defects such as Ti interstitials may play an equally important role in these processes. Unfortunately, there still exist too many unknowns (for example, the identity of X) for us to gain a firm handle on the effect of O_2 quenching and Al doping.

IV. THEORY

In Sec. III, we proposed a model to account for the observed EPR spectra. In this section, we shall discuss the theoretical details of this model, of which the most striking feature is the sharing of a hole among the six oxygen ions surrounding a Ti^{4+} site. This implies overlap between individual oxygen atomic wave functions—a very probable situation since evidence exists that the oxygen octahedron in SrTiO₃ is a tightly bound unit. This has been demonstrated by the observation of two soft (low-frequency) phonon modes in

---

[31] R. A. Forman (unpublished).

SrTiO$_3$.[2,3] One of these is a rotation of the oxygen octahedra while the other is primarily a vibration of the Ti ion against the surrounding oxygen octahedron. In both these modes, it is the O$_6$ octahedron which retains its identity. Thus, in some sense, these octahedra can be considered the basic building blocks of the SrTiO$_3$ crystal.

By assuming sharing of the hole among the oxygens, we retain the full O_h symmetry of the titanium site. In the tetragonal phase, the deviation from O_h symmetry is small,[13] and we shall neglect it in the first approximation. The symmetry at the oxygen site is D_{4h}, and, thus, the triply degenerate p states of the oxygen ions are split into σ and π states. The six oxygens with their p orbitals give rise to 6 σ and 12 π states. The linear combinations of oxygen $2p$ atomic orbitals appropriate for O_h symmetry are presented in Table IV. The subscripts on the p orbitals refer to the individual oxygen ions, labeled as shown in Fig. 6. Only one component of the triplet states is given; the others can be obtained by a permutation of the axes. In writing these wave functions, overlap between the $2p$ functions of different oxygen ions has been neglected. Inclusion of overlap terms, however, would only change the normalization factors, not the symmetry properties. Finally, the molecular orbital states of Table IV are depicted in Fig. 7, where the arrows illustrate the positive sense of the p functions.

Important to this model are the overlap integrals which account for the sharing and which determine the energies of the states. There are two types of overlap terms. First, we have the direct overlap
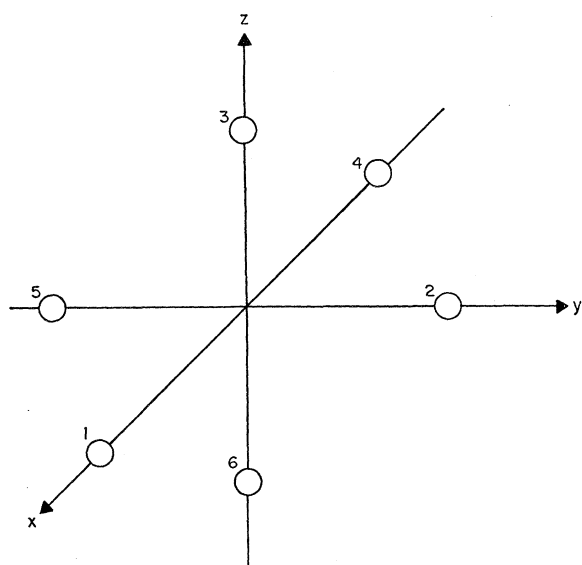
$$S_{lm}(i,j) = \langle p_l(i) | p_m(j) \rangle,$$

where l and m refer to particular oxygen ions and i and j represent the components of the oxygen p-orbitals. The second overlap integral is

$$H_{lm}(i,j) = \langle p_l(i) | \mathcal{3C} | p_m(j) \rangle,$$

where $\mathcal{3C}$ is the one-electron Hamiltonian. The energies of the molecular orbital states are determined by solving the secular equation[32]

$$|H_{lm}(i,j) - S_{lm}(i,j)E| = 0.$$

Considering overlap only between neighbors, we note that the overlap integrals are usually largest when the p orbitals are directed toward, rather than parallel to, each other. For instance, $H_{12}(y,x)$ is expected to be larger than $H_{12}(z,z)$. Thus, by inspecting Fig. 7, we can estimate which states are likely to lie lowest. Depending upon the sign of the overlap terms, the possible ground states include; t_{2g} or t_{1g} (π states), a_{1g} or e_g (σ states).

TABLE IV. Linear combinations of oxygen $2p$ atomic orbitals appropriate for O_h symmetry.

States	Symmetry	Wave function
σ	a_{1g}	$\psi = (\frac{1}{6})^{-1/2}[\,|x_1\rangle + |y_2\rangle + |z_3\rangle - |x_4\rangle - |y_5\rangle - |z_6\rangle\,]$
σ	t_{1u}	$\psi_z = (2)^{-1/2}[\,|z_3\rangle + |z_6\rangle\,]$, etc.
σ	e_g	$\psi_{z^2} = \frac{1}{6}\sqrt{3}[2\,|z_3\rangle - 2\,|z_6\rangle - |x_1\rangle - |y_2\rangle + |x_4\rangle + |y_5\rangle\,]$
		$\psi_{x^2-y^2} = \frac{1}{2}[\,|x_1\rangle - |y_2\rangle - |x_4\rangle + |y_5\rangle\,]$
π	t_{2g}	$\psi_z = \frac{1}{2}[\,|y_1\rangle + |x_2\rangle - |y_4\rangle - |x_5\rangle\,]$, etc.
π	t_{1u}	$\psi_z = \frac{1}{2}[\,|z_1\rangle + |z_2\rangle + |z_4\rangle + |z_5\rangle\,]$, etc.
π	t_{1g}	$\psi_z = \frac{1}{2}[\,|y_1\rangle - |x_2\rangle - |y_4\rangle + |x_5\rangle\,]$, etc.
π	t_{2u}	$\psi_z = \frac{1}{2}[\,|z_1\rangle - |z_2\rangle + |z_4\rangle - |z_5\rangle\,]$, etc.

Deciding whether the hole is in a π state or σ state is not aided by intuition. In the absence of any neighboring defects, the π orbitals of an oxygen ion are of lower energy for a hole than the σ orbitals. However, since in our case a hole is trapped by a charge defect at the Ti site, we would expect the energy of the σ orbital to be lowered. Fortunately, by proceeding to a consideration of g values, we can determine whether a σ or a π state is the ground state for the hole.

The ground state must have an almost isotropic g value near the spin-only value of 2.0023. Thus, the orbital angular momentum is quenched. For the orbital triplet states, however, such a large quenching of the angular momentum almost always implies a deviation from cubic symmetry of a sizeable Jahn-Teller[33] effect. As a result, if a triplet state has a g value near 2, it would be anisotropic; or, if isotropic, the g value would not be near 2. This argument allows us to eliminate the π states as possible ground states.

FIG. 6. Labeling of coordinate system and oxygen ions in O_h symmetry.

[32] P. O. Löwdin, J. Chem. Phys. 18, 365 (1950).
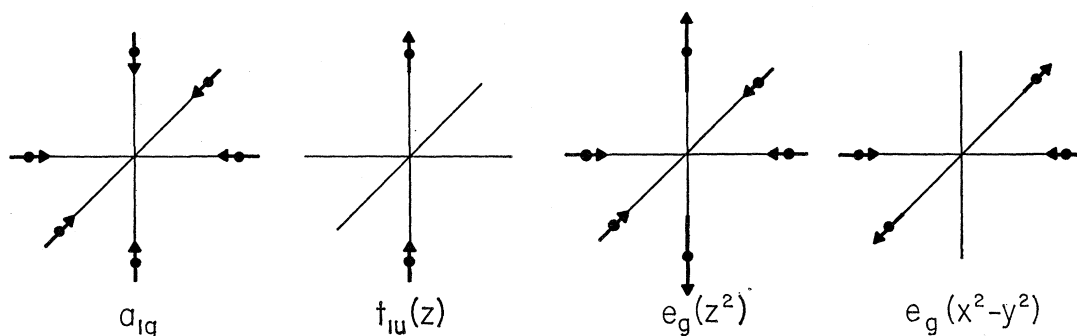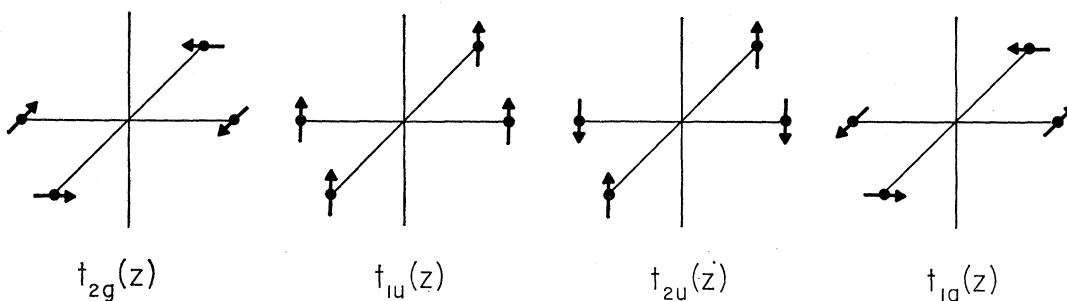[33] F. S. Ham, Phys. Rev. 138, A1727 (1965); 160, 328 (1967).

(a) σ ORBITALS

(b) π ORBITALS

FIG. 7. The σ and π molecular orbital states in O_h symmetry. The arrows represent the p orbitals of the oxygens.

The hyperfine structure of the Al-O⁻ center can be used to determine whether the hole exists in a ^2e_g or $^2a_{1g}$ state. The hyperfine splitting depicted in Fig. 3 follows an $A_s + A_p(3\cos^2\theta - 1)$ dependence, where θ is the angle between the external magnetic field and a [001] axis. Values of $A_s = 7.8 \times 10^{-4}$ cm⁻¹ and $A_p = 0.2 \times 10^{-4}$ cm⁻¹ have been obtained from the experiment. Since the isotropic contribution to the hyperfine interaction dominates (i.e., $A_s \gg A_p$), the major portion of the hyperfine splitting arises from the contact term. For Al²⁺, the magnitude of the direct hyperfine interaction for the $3s$ electron is the order of 450×10^{-4} cm⁻¹. This is 50 times the magnitude of A_s for the Al-O⁻ center and implies that we are observing a super-hyperfine interaction with a mixing coefficient of about $1/7$. The only molecular orbital state which has direct mixing with the aluminum $3s$ state is $^2a_{1g}$. A hole in the ^2e_g state could give rise to an isotropic superhyperfine coupling by means of configurational mixing to the $^2a_{1g}$ state. In this case, however, A_s is expected to be much smaller than the measured value. Thus, the evidence implies that the $^2a_{1g}$ molecular state is the ground state of the Al-O⁻ center.

The anisotropic contribution to the superhyperfine interaction A_p is small; however, its origin if of interest.

Displacement of the aluminum nucleus slightly off-center would admix some $^2t_{1u}$ state into $^2a_{1g}$. With the hole partially in a p state, overlap with the $2p$ or $3p$ state of the Al ion would be expected. In addition, there would be a dipole-dipole contribution of order $\gamma_h\gamma_{Al}/R^3$, where γ_h and γ_{Al} are the nuclear magnetic moments of the hole and aluminum nucleus, respectively.

Let us now consider the g shift which is expected for a hole in the $^2a_{1g}$ state. Normally, the expression

$$\Delta g_i = 2\lambda \sum_n \frac{\langle \psi_0 | L_i | \psi_n \rangle \langle \psi_n | L_i | \psi_0 \rangle}{E_n - E_0}$$

is used, where $i = x$, y, or z. However, this calculation is complicated by the many-ion character of our center. Fortunately, this problem has been considered before in the theories of the F and the V_k centers in the alkali halides (see Ref. 34). It has been shown that the angular momentum can be taken about each oxygen

---

[34] F. J. Adrian, Phys. Rev. **107**, 488 (1957); J. J. Markham, *F-Centers in Alkali Halides* (Academic Press Inc., New York, 1966), pp. 202–205 and 212–219; C. P. Slichter, *Principles of Magnetic Resonance* (Harper and Row Publishers, Inc., New York, 1963), pp. 201–215.

ion separately. Therefore,

$$\Delta g_i = 2\lambda \sum_n \sum_k \frac{\langle \psi^0 | l_i(k) | \psi_n \rangle \langle \psi_n | l_i(k) | \psi_0 \rangle}{E_n - E_0},$$

where $l_i(k)$ refers to the ith component of angular momentum about the kth ion. Applying this expression to the $^2a_{1g}$ state, we obtain

$$\Delta g = \tfrac{4}{3}\lambda / [E(^2t_{1g}) - E(^2a_{1g})],$$

from experiment, $\Delta g = 0.011$, and $\lambda = 135$ cm^{-1} from extrapolation of the spin-orbit parameter of the $2p^5$ isoelectronic series, F I to S VIII.[35] Thus, $E(^2t_{1g}) - E(^2a_{1g}) = 16\,300$ cm^{-1}. This is a reasonable value considering that the $^2t_{1g}$ state should be at a higher energy than the $^2t_{1u}$ or $^2t_{2u}$ states. The energy of the odd states is estimated to be about 12 500 cm^{-1}, assuming that the measured optical absorption at 800 nm corresponds to a transition from the even ground state to an odd excited state.

The tetragonal character of the Al-O$^-$ EPR spectrum is possibility associated with a displacement of the Al^{3+} ion alone one of the cubic axes. The anitotropy of the g value is about 10% of the g shift, and could result from either a splitting of the $^2t_{1g}$ state or from mixing of the $^2a_{1g}$ state with $^2t_{1u}(\sigma)$. The latter is probably more important because the superhyperfine splitting also has an anisotropic component, and the $^2t_{1g}$ state admixes very little with the Al^{3+} states. In conclusion, our proposed model describes the Al-O$^-$ center very well. Therefore, we shall use this model as the basis for discussing the X-O$^-$ center in light of the similarity of these centers.

At this point, we shall discuss in greater detail two candidates for the X-O$^-$ center which were proposed in Sec. III. The first possibility was that this center is merely another state of the Al-O$^-$ center. The main evidence for this idea is that the concentration of X-O$^-$ centers is proportional to aluminum doping. The

absence of hyperfine structure in the X-O$^-$ spectrum could be accounted for by placing the hole in a non-bonding π state. The measured g value, however, implies that the hole cannot reside in a π state. In order for an orbital triplet state to have a g near two, the angular momentum **L** must be quenched. One way of quenching **L** is by a low-symmetry crystalline field, but then the g value would be anisotropic. **L** can also be quenched by a Jahn-Teller effect, which is equivalent to a low-symmetry distortion. However, in this case, the anisotropy would be averaged by allowing for relaxation between the Jahn-Teller states. On the other hand, this relaxation should be temperature-dependent, and, at low temperatures, the relaxation should increase sufficiently to provide an anisotropic spectrum. This is not observed down to 4.2°K.

A second possibility was that X (in the X-O$^-$ center) is a defect different from Al^{3+}. We have observed that the X-O$^-$ center retains cubic symmetry and is more stable than the Al-O$^-$ center. Thus, a larger charge deficiency would seem likely, such as a titanium vacancy. Such a defect, however, implies a larger central field acting on the oxygen octahedron. We would expect, therefore, that the separation between the σ and π states would increase. This, in turn, would affect the g shift, unless there is a compensating change in the spin-orbit coupling. As we have seen, the g shift of the X-O$^-$ center is nearly identical with that of the Al-O$^-$ center. In conclusion, each of the above proposed models for the X-O$^-$ center agrees with some of the experimental data, but not with all of it. The origin of the X-O$^-$ center still remains a mystery.

ACKNOWLEDGMENTS

---

[35] C. E. Moore, Natl. Bur. Std. (U. S.) Circ. No. 467 (1949), Vol. I.